DESERT 2022, 27(1): 153-166
DOI: 10.22059/JDESERT.2022.88520

RESEARCH PAPER

Comparative study of aerosol optical depth satellite data with earth's observations

Mohsen Araghizadeh[1], Sayed Abolfazl Masoodian[1,*]

[1]Faculty of Geographical Sciences and Planning, University of Esfahan, Esfahan, Iran

Received: 1 December 2021, Revised: 28 December 2021, Accepted: 2 February 2022

Abstract
This research seeks to investigate the consistency of satellite data and the information obtained from the ground meteorological stations in Iran. In this study, the Aerosol Optical Depth (AOD) data of Moderate Resolution Imaging Spectroradiometer (MODIS) deep blue algorithm of Terra satellite from 2000-2018 was used. The data of 390 meteorological stations during2000-2018 were used to evaluate and validate the satellite data. The aerosol optical depth (AOD) was studied and compared with the current weather codes of meteorological stations (codes 00 to 99). The frequency percentage and spatiotemporal matching methods were further used. Based on the results, the AOD at 550 nm data of the Terra satellite MODIS sensor had a significant relationship with the meteorological codes of 00 to 99 in Iran. This topic is useful in the study of meteorological phenomena. The present study evaluated the large values of aerosol optical depth (AOD) of meteorological phenomena in the boundary layer. The highest frequency percentage of the aerosol optical depth (AOD) between 0 and 3.5 belonged to the present weather codes No. 5 and 6. The amount of aerosol optical depth (AOD) was directly related to meteorological phenomena (short- or long-term) such as natural, industrial, and urban pollution, smoke, humidity changes, lightning, thunderstorms, and heavy rainfall. The amount of aerosol optical depth (AOD) varied depending on the season, place, and meteorological phenomena in Iran.
Keywords: Aerosol optical depth, MODIS, Deep blue, Present weather, Iran.

Introduction

Satellite data and remote sensing are greatly useful and practical for studying aerosols, and it is necessary to identify pollution in different parts of the country. The present study aimed to investigate and correlate the Aerosol Optical Depth (AOD) data with the present weather (WW) phenomena reported by ground meteorological stations. Data validation was performed to ensure the use of MODIS Aerosol Optical Depth (AOD). The use of long-term series of satellite data from 2000 to 2018 and the application of 390 ground meteorological stations in eight synoptic observation times are among the innovations of this research. Ground meteorological station data allows for addressing aerosol optical depth data and its accuracy in tracking meteorological phenomena such as dust storms.

Kaufman et al.(1997) considered MOSID aerosol data for studying dust climatology and identifying dust sources and subsidence places along with different types of aerosols. Thomas et al.(2019) used MODIS AOD data in a 10-year study on the North Pole to study atmospheric column aerosols in atmospheric stability and temperature inversion at the boundary layer in different seasons. Gkikas et al.(2009) introduced the AOD threshold with a formula and studied spring, summer, autumn, and winter seasons. Based on the results, values greater than the aerosol optical depth threshold belonged to dust particles (soil) while those less than the AOD threshold were related to sea salt, fossil fuel particles, forest fires, and

* Corresponding author e-mail: s.a.masoodian@geo.ui.ac.ir

human activities. Wahab et al.(2014) used MODIS satellite and aerosol optical depth (AOD) data in Hong Kong in the period from 2006 to 2011 and applied AERONET ground data for verification. AOD has two algorithms, namely Dark Target (DT) and Deep Blue (DB) (MODIS Portal, 2021). Hsu et al.(2013) reviewed deep blue data from 1997 to 2010 comparing and validating it with AERONET ground data. Klingmüller et al.(2016) examined and explained the trend of dust concentration in the Middle East during the period from 2000 to 2015using the data from the DB and DT algorithms of MODIS Aerosol Optical Deep (AOD) product. Sayer et al.(2013) applied the C6 products of the MODIS Aerosol Optical Depth (AOD) Deep Blue (DB) algorithm and utilized data from 60 AERONET stations around the world for validation. They concluded that the deep blue C6 data is of high quality and suitable for the study of desert areas and bright surfaces. In China, Wei et al. (Wei & San, 2016) used the DB and DT algorithm data from MODIS C5 and C6 categories as well as their combinations (DT&DB) and validated them using the data from four AERONET stations in 2013 and 2014. They reported a good correlation between DB and AERONET. Fan et al.(2017) surveyed different regions of China with MODIS satellite data from 2001 to 2015 and validated the data with 16 AERONET ground stations. Bilal et al.(2018) utilized the data obtained from DB and DT algorithms and their combination in Europe from 2008 to 2012 and verified them with the help of 19 AERONET ground stations in Europe. Using the deep blue data of MODIS Terra satellite aerosol optical depth (AOD) for quantitative research and processing has suggested and highlighted by Sayer et al. (2015). Levy et al. (2010 and 2013) used MODIS AOD data from C5 and C6 datasets with DB and DT algorithms in a comprehensive global review. Wei et al.(2020) validated AOD data (MOD04_3K) from 2013 to 2017 with 384 stations on land and ocean and AERONET version 3 finding a major correlation between satellite data and ground data. Level 2 data of AERONET is used in almost all studies that apply AERONET data to obtain characteristics or evaluate other methods (Bahram Vash Shams and Mohammadzadeh, 2013). Levy et al. (2010) used more than 300 AERONET ground stations for validation and revealed a high correlation between MODIS and AERONET data. Li et al.(2021) conducted remote sensing research on the Taklamakan Desert in China and the results of MODIS aerosol products (MCD19A2) were compared and verified with the CE-318 solar radiometer data. The MODIS Aqua satellite AOD data with a resolution of 10 km and NPP-VIIRS AOD data with a resolution of 6 km were compared and validated with AERONET AOD data from 2013 to 2018 in different regions of China (Wei et al., 2018). In Iran, Raigani and Kheirandish, (2017) studied the aerosol optical depth (AOD) in Alborz province and recognized the dust centers of Alborz province using a time series of remote sensing data. The results of their study were validated with the ground-based dust data from meteorological stations and air pollution monitoring. Soleimani et al. (2015) highlighted the importance of knowing the aerosols in the Persian Gulf and reviewed the AOD data in the Persian Gulf region from March 2008 to December 2013. In their work, the data of Aqua and Terra satellites along with the particulate matter (PM10) data of environmental stations and AOD of AERONET stations were used to evaluate the aerosol optical depth. Based on their findings, the AOD data of the MODIS sensor was of acceptable accuracy and there was a high correlation between the values measured and the AERONET network. Besides, Soleimani emphasized that the aerosol optical depth (AOD) data of the MODIS sensor provided accurate information on the amount of fine-grained dust in the Persian Gulf region.

Their results and calculations indicated that the optical thickness τ at 550 nm was useful for measuring the fabricated smoke and urban pollution (Kaufman et al., 2005). Using the following formula, the final product of column mass concentration is calculated, which is a combination of fine and coarse particle models and the mass concentration coefficient of each particle ($M = \tau^f M_c^f + \tau^c M_c^c$) (Levy et al., 2009). Remer et al.(2005) investigated MODIS

aerosol sensor and showed the distribution of fine particles (such as smoke particles and industrial and fabricated pollutants) and coarse particles (such as desert sand, dust, and sea salt). While showing that coarse particles have larger AODs and fine particles have smaller AODs, they concluded that MODIS sensor data is effective and useful for detecting natural and fabricated particles and aerosols. Alam et al. (2010) evaluated the daily Level-3 MODIS aerosol optical depth data of the MODIS Terra satellite in eight cities of Pakistan from 2001 to 2006 and surveyed the AOD of suspended particles and the pollutants of the boundary layer and clouds with an annual time series. The coordination of AOD with the amount of water vapor in the atmosphere was among their most important results. They further found an increase in AOD in the coastal and southern parts of Pakistan during the summer and wet seasons. Levy introduced low values and AOD=0.0 for atmospheric molecular particles (Rayleigh scattering) where AOD>0.0 indicated aerosols (suspended particles), atmospheric particles, and gases (Levy et al., 2013). The lightning phenomenon was also investigated in the study of Kucienska (Kucienska et al., 2013) with AOD value. They used the MODIS data and the data from the World-Wide Lightning Location Network (WWLLN) in 2007 and concluded that lightning and AOD had a positive relationship in land and coastal areas. In China, Xin et al. (2016) compared the PM2.5 levels of pollutants from different regions with the AOD data of the MODIS sensor and showed a good correlation and linear relationship between pollutants and AOD. Through examining the urban, industrial, and desert areas of China with statistical calculations, Wei et al. (2018) believed that AOD values greater than 1 indicated severe pollution in the cities of Beijing, Tianjin, and Hebei. Ichoko et al.(2004) used monthly and daily long-term time series of AOD in the northern and southern hemispheres and selected different cities of the world. They used AOT values, effective particle radius, and Angstrom index of the MODIS Layer 2 data series with a resolution of 10 km from 2000 to 2002 and examined various boundary layer pollutions and atmospheric phenomena such as atmospheric suspended pollutants, smoke, dust, and sea salt in land and ocean. Ensafi Moghadam, T. (2020) studied the phenomenon of dust in seven western provinces of Iran. For this purpose, she used the MODIS deep blue data from 1996 to 2016 and validated them with ground meteorological station data. Based on the results, Ensafi Moghadam mentioned the compatibility of satellite data and meteorological data.

Materials and Methods

Study area

The current study focused on the cities and meteorological stations of Iran (Figure 1). Iran is an arid and semi-arid country in West Asia with an area of more than 1648,000 square kilometers. Considering the wind, atmospheric humidity, and temperature, Masoodian (2011) divided Iran into eight climatic regions according to their geographical location:1. Highland climate, 2. Western foothill climate, 3. Climate of the Persian Gulf coast, 4. Climate of the northern slopes of Alborz, 5. Climate of the Caspian coast,6. Eastern foothills climate,7. Eastern plateau climate, and 8. Oman coastal climate. This division provides a good perspective for dust distribution areas in Iran as areas 3, 6, 7, and 8 are the main dust areas in Iran.

Data

In this research, we used two types of data from 2000 to 2018.

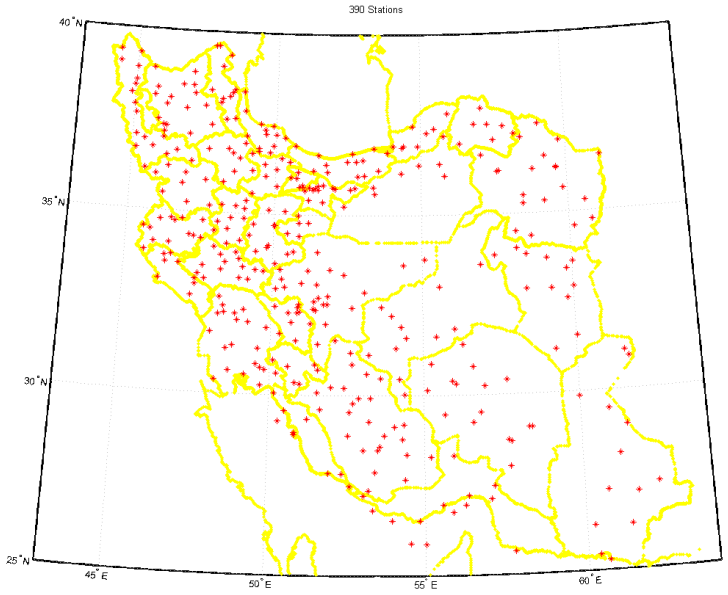

Figure 1. Location of 390 synoptic meteorological stations

Synoptic meteorological stations of the Meteorological Organization of Iran

The mentioned data was derived from the database of the Meteorological Organization (https://irimo.ir/far/index.php) on a daily basis. Information included codes 00 to 99 of the present weather of 390 meteorological stations based on 8 times of synoptic monitoring. Data were prepared for 390locationsof synoptic meteorological stations and the period from 2000 to 2018. Note that the 6861*390 *8 matrix gives the number of days in an 18-year period, the number of stations, and the turn of the synoptic observation, respectively. Figure 1 illustrates the location of the stations used in this study. Table 1 defines the present weather codes for synoptic monitoring stations.

Table 1. Present weather WMO† codes 00 to 99

00	Cloud development not observed or not observable	50	Drizzle, not freezing, intermittent, slight at time of ob.
01	Cloud generally dissolving or becoming less developed	51	Drizzle, not freezing, continuous, slight at time of ob.
02	State of sky remaining unchanged on the whole	52	Drizzle, not freezing, intermittent, moderate at time of ob.
03	Clouds generally forming or developing	53	Drizzle, not freezing, continuous, moderate at time of ob.
04	Visibility reduced by smoke, e.g. veldt or forest fires, industrial smoke or volcanic ashes	54	Drizzle, not freezing, intermittent, heavy at time of ob.
05	Haze	55	Drizzle, not freezing, continuous, heavy at time of ob.
06	Widespread dust in suspension in the air, not raised by wind at or near the station at the time of observation	56	Drizzle, freezing, slight
07	Dust or sand raised by wind at or near the station at the time of observation, but not well-developed dust whirl(s) or sand whirl(s), and no dust storm or sandstorm seen; or, in the case of ships, blowing spray at the station	57	Drizzle, freezing, moderate or heavy (dense)

† World Meteorology Organization

Continued Table 1. Present weather WMO codes 00 to 99

08	Well-developed dust or sand whirl(s) seen at or near the station during the preceding hour or at the time of observation, but no dust storm or sandstorm	58	Rain and drizzle, slight
09	Dust storm or sandstorm within sight at the time of observation, or at the station during the preceding hour	59	Rain and drizzle, moderate or heavy
10	Mist	60	Rain, not freezing, intermittent, slight at time of ob.
11	Patches of shallow fog or ice fog at the station, whether on land or sea not deeper than about 2 meters on land or 10 meters at sea	61	Rain, not freezing, continuous, slight at time of ob.
12	More or less continuous shallow fog or ice fog at the station, whether on land or sea, not deeper than about 2m/land or 10m/sea	62	Rain, not freezing, intermittent, moderate at time of ob.
13	Lightning visible, or thunder heard	63	Rain, not freezing, continuous, moderate at time of ob.
14	Precipitation within sight, not reaching the ground or the surface of the sea	64	Rain, not freezing, intermittent, heavy at time of ob.
15	Precipitation within sight, reaching the ground or the surface of the sea, but distant, i.e. > 5 km from the station	65	Rain, not freezing, continuous, heavy at time of ob.
16	Precipitation within sight, reaching the ground or the surface of the sea, close to, but not at the station	66	Rain, freezing, slight
17	Thunderstorm, but no precipitation at the time of observation	67	Rain, freezing, moderate or heavy
18	Squalls at or within sight of the station during the preceding hour or at the time of observation	68	Rain or drizzle and snow, slight
19	Funnel clouds at or within sight of the station during the preceding hour or at the time of observation	69	Rain or drizzle and snow, moderate or heavy
20	Drizzle (not freezing) or snow grains, not falling as showers, during the preceding hour but not at the time of observation	70	Intermittent fall of snowflakes, slight at time of ob.
21	Rain (not freezing), not falling as showers, during the preceding hour but not at the time of observation	71	Continuous fall of snowflakes, slight at time of ob.
22	Snow, not falling as showers, during the preceding hour but not at the time of observation	72	Intermittent fall of snowflakes, moderate at time of ob.
23	Rain and snow or ice pellets, not falling as showers; during the preceding hour but not at the time of observation	73	Continuous fall of snowflakes, moderate at time of ob.
24	Freezing drizzle or freezing rain; during the preceding hour but not at the time of observation	74	Intermittent fall of snowflakes, heavy at time of ob.
25	Shower(s) of rain during the preceding hour but not at the time of observation	75	Continuous fall of snowflakes, heavy at time of ob.
26	Shower(s) of snow, or of rain and snow during the preceding hour but not at the time of observation	76	Diamond dust (with or without fog)
27	Shower(s) of hail, or of rain and hail during the preceding hour but not at the time of observation	77	Snow grains (with or without fog)
28	Fog or ice fog during the preceding hour but not at the time of observation	78	Isolated star-like snow crystals (with or without fog)
29	Thunderstorm (with or without precipitation) during the preceding hour but not at the time of observation	79	Ice pellets
30	Slight or moderate dust storm or sandstorm - has decreased during the preceding hour	80	Rain shower(s), slight

Continued Table 1. Present weather WMO codes 00 to 99

31	Slight or moderate dust storm or sandstorm - no appreciable change during the preceding hour	81	Rain shower(s), moderate or heavy
32	Slight or moderate dust storm or sandstorm - has begun or has increased during the preceding hour	82	Rain shower(s), violent
33	Severe dust storm or sandstorm - has decreased during the preceding hour	83	Shower(s) of rain and snow, slight
34	Severe dust storm or sandstorm - no appreciable change during the preceding hour	84	Shower(s) of rain and snow, moderate or heavy
35	Severe dust storm or sandstorm - has begun or has increased during the preceding hour	85	Snow shower(s), slight
36	Slight/moderate drifting snow - generally low (below eye level)	86	Snow shower(s), moderate or heavy
37	Heavy drifting snow - generally low (below eye level)	87	Shower(s) of snow pellets or small hail, with or without rain or rain and snow mixed - slight
38	Slight/moderate blowing snow - generally high (above eye level)	88	Shower(s) of snow pellets or small hail, with or without rain or rain and snow mixed - moderate or heavy
39	Heavy blowing snow - generally high (above eye level)	89	Shower(s) of hail, with or without rain or rain and snow mixed, not associated with thunder - slight
40	Fog or ice fog at a a distance at the time of observation, but not at station during the preceding hour, the fog or ice fog extending to a level above that of the observer	90	Shower(s) of hail, with or without rain or rain and snow mixed, not associated with thunder - moderate or heavy
41	Fog or ice fog in patches	91	Slight rain at time of observation - Thunderstorm during the preceding hour but not at time of observation
42	Fog/ice fog, sky visible, has become thinner during the preceding hour	92	Moderate or heavy rain at the time of observation - Thunderstorm during the preceding hour but not at time of observation
43	Fog/ice fog, sky invisible, has become thinner during the preceding hour	93	Slight snow, or rain and snow mixed or hail at time of observation - Thunderstorm during the preceding hour but not at time of observation
44	Fog or ice fog, sky visible, no appreciable change during the past hour	94	Moderate or heavy snow, or rain and snow mixed or hail at time of observation - Thunderstorm during the preceding hour but not at time of observation
45	Fog or ice fog, sky invisible, no appreciable change during the preceding hour	95	Thunderstorm, slight or moderate, without hail, but with rain and/or snow at time of observation
46	Fog or ice fog, sky visible, has begun or has become thicker during preceding hour	96	Thunderstorm, slight or moderate, with hail at time of observation
47	Fog or ice fog, sky invisible, has begun or has become thicker during the preceding hour	97	Thunderstorm, heavy, without hail, but with rain and/or snow at time of observation
48	Fog, depositing rime, sky visible	98	Thunderstorm combined with dust/sandstorm at time of observation
49	Fog, depositing rime, sky invisible	99	Thunderstorm, heavy with hail at time of observation

Aerosol optical depth data of MODIS Terra satellite

The AOD (550 nm) data of MODIS deep blue with a spatial resolution of 10 km can be used on vegetated surfaces, urban areas, and arid areas and is suitable for quantitative use in scientific applications. This data has been calculated and processed in cloudless conditions without ice and snow surfaces. It is particularly useful for studying different types of aerosols, and small and large particles (Hsu et al., 2013). Regarding the reflectance at 550 nm, the lowest values belong to water, vegetation, and clouds while the highest values are related to snow. The MODIS deep blue data correct the vegetation, snow, and clouds. Therefore, it can be said that the highest amount of signal transmission to the end of the atmosphere occurs at this frequency. On the other hand, MODIS uses the VIS and near-infrared (NIR) vision band to study the column of particles and materials from the ground to the top of the atmosphere, and AOD values accurated and acceptable. The removal of clouds and correction of bright surfaces (such as deserts and snow-covered surfaces) and water areas are but some of the benefits of using the MODIS 550 nm channel (Chu et al., 2003).

Scientific data of the MOD04_L2 product are stored in HDF format (MODIS Portal, 2021). In the present study, the MODIS aerosol data (unitless) mounted on the Terra satellite was used and the scientific specification (10KM) wasV61 MOD04-L2. Deep_Blue_Aerosol_Optical_ Depth_550_Land data was further used. Other researchers have validated deep blue data to study atmospheric aerosols (Sayer et al., 2015), and the spatial resolution of this data is 10 km. Terra satellite data is available daily for every 5 minutes. The period of data in this research was from 2000/03/20 to 2018/12/31, which is about 18 years (6761 days).

After storing the mentioned folders from 2000 to 2018, several daily files (about 28470 files) were integrated with the help of MATLAB software (R2014a) and the data were converted into real values via applying coefficients. By use of MATLAB programming (R2014a) software and interpolation, the spatial correction was performed and only the cell data in the mainland of Iran were selected, and the geographical coordinates of the satellite data were also determined. Accordingly, the data were converted into a daily file with significant geographical coordinates. It is worth noting that the most accurate satellite data and the closest cell (pixel) to the meteorological station should be selected to prepare the data. In this regard, the time series of satellite data and average AOD are prepared and calculated for each station in the optimal best network cell. For more accuracy, it is necessary to select the location of each cell and meteorological station to its minimum value. This selection will verify the satellite data at each meteorological station. Based on the results, the time-location matrix obtained for AOD was 6861×390, where6861 (time) value indicates the number of studied days (about 18 years) and 390 (location) value gives the number of meteorological stations distributed throughout the country.

Frequency percentage of aerosol optical depth (AOD_{550})

By calculating the frequency of phenomena (codes 0 to 99) in Table 2, 06GMT selects the best observation time and the frequency percentage of all meteorological phenomena calculated at this time.

Table 2. Frequency of codes 00 to 99 and 8 synoptic monitoring times

TIME / Code	GMT 00	GMT 03	GMT 06	GMT 09	GMT 12	GMT 15	GMT 18	GMT 21
WW=[00:99]	198,863	447,829	481,766	403,939	412,076	400,096	214,980	183,473
WW=[6:9,30:35]	21,832	60,406	80,153	93,853	96,970	81,907	29,993	24,461
WW=~[6:9,30:35]	177,031	387,423	401,613	310,086	315,106	318,189	184,987	159,012
WW=[30:35]	101	320	583	395	334	280	98	98

In the AOD matrix of the 18-year statistical period, the frequency of the aerosol optical depth (AOD) is classified in steps of 0.1 ($cls = [0: 0.1: 3.5]$) and the frequency of each class is calculated during the statistical period. Using the following formulas and calculations, the frequency and frequency percentage of the two states with and without dust storms are obtained.

$$P = \frac{F}{SF} * 100 \quad (1)$$

F: Frequency of classified AOD values in 6861 days
SF: Sum of the frequency of all classes of AOD values in 6861 days
P: Frequency percentage of classified AOD values in 6861 days

The following formula determines difference between the frequency percentage of the aerosol optical depth (AOD)with and without dust storm.

$$R = \mathbf{P_{Dust}} - \mathbf{P_{No\ Dust}} \quad (2)$$

The horizontal axis represents the classified AOD values while the vertical axis indicates the difference in the frequency percentage of AOD with and without dust storms.

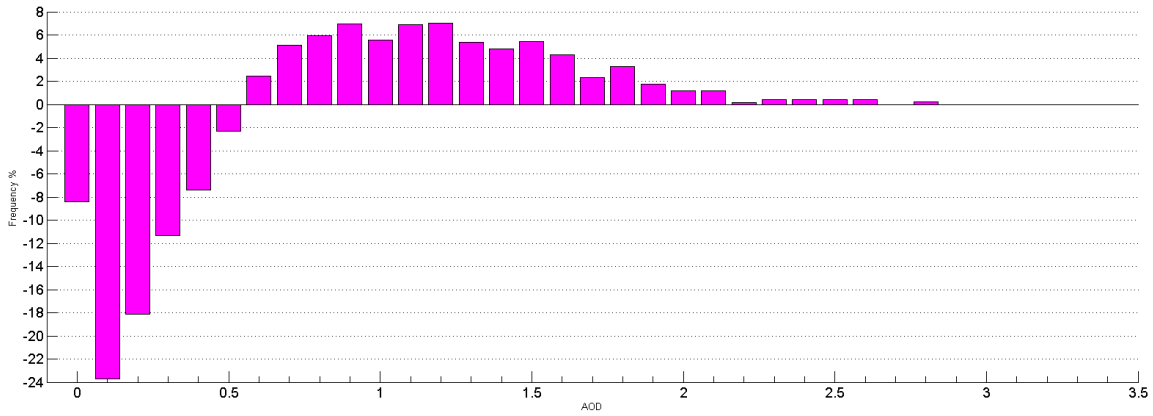

Figure 2. Frequency distribution of dust storm and non-dust storm conditions

As shown in Figure 2, the values from 0 to 3.5 of the aerosol optical depth (AOD) are significant. The first and second parts are the aerosol optical depth (AOD) without and with dust storm (codes 30 to 35) and the aerosol optical depth (AOD) is revealed from the 0.6 category and continues up to 2.8. The AOD values higher than 2.8 are not related to the occurrence of dust storms, but other weather phenomena. Dust storms with winds of 18.5 m/s, horizontal visibility of 100 m, relative humidity of 12.5%, and aerosol optical depth (AOD) up to 2.8 have been reported in Zahak, Zabol, and Miandoab cities. However, it is important to study other meteorological phenomena for the correct validation of AOD values.

Table 3. Percentage of aerosol optical depth (AOD) and present weather codes (WW) (at 06 GMT)

WW codes	4	5	10	64	91	95
Frequency Percentage	0.47	63.11	20	0.03	8.33	0.74
AOD class	0/2-0/3	0/2-0/3	0-0/1	1/0-1/1	2/9-3/0	1/9-2/0

Table 3 gives the frequency percentage of aerosol optical depth (AOD) of important meteorological phenomena. The details of the codes in this table are as follows:
Code 4: Industrial smoke, forest fires, or volcanic ash

Code 5: Solid and suspended particles such as smoke, water vapor, pollution, or fine sand particles
Code 10: Water vapor and steam caused by fine water particles suspended in the air
Code 64: Heavy non-frozen rain
Code 91: Gentle rainstorm with lightning in the last hour
Code 95: Lightning with light to moderate snow and rain

Results and Discussion

Daily survey of meteorological stations shows that several phenomena and codes were reported in a station in one day, all of which had to be considered simultaneously. For example, the city of Ilam reported heavy snow and fog on 2017/2/2 while the city of Jolfa experienced thunderstorms, rainstorms, and light rainstorms on 2009/1/27. Table 3 shows the highest frequency of aerosol optical depth (AOD) for each code. The frequency 0.47% of AOD 0.2 to 0.3 was with observation code number 4 which happened more in June and July. This phenomenon was more common in the northwest, west, and southwest of Iran. The AOD>0.3 (0.3 of average value) in June and July was higher than that of other months of the year. The city of Hassanabad Darab (Fars) had a value of AOD 1.1 on 2011/06/26, which had a code of 5 in the previous hours. The highest number of AOD belonged to code 4 with a value of 1.41 in the city of Marivan on 2003/07/07, which may have been caused by the burning of chemicals and sulfur in Iraq (Baghdad) at that time. According to scientific studies (Alam et al., 2010), the transfer of industrial and urban pollution from other areas and sources is possible, and the migration of pollutants to the city of Marivan may have increased the amount of AOD.
Factory pollution in industrial and large cities, humidity in the atmosphere, air stability, and accumulation of pollutants will increase the amount of AOD, which is consistent with scientific research (Chu et al., 2003). Code 5 had the most observations. 63.11% of 0.2<=AOD<=0.3 is in code 5 (Table 3). This phenomenon (HAZE) existed in all parts of the country and there was a frequency of 57.1% of large 3.4<=AOD<=3.5 with code 5.

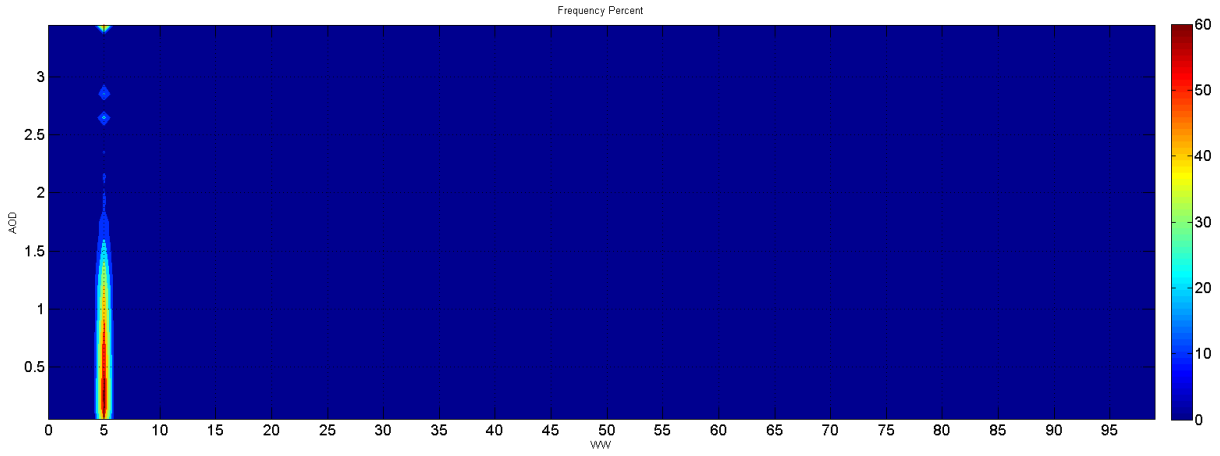

Figure 3. Frequency percentage of aerosol optical depth (AOD) in code 5

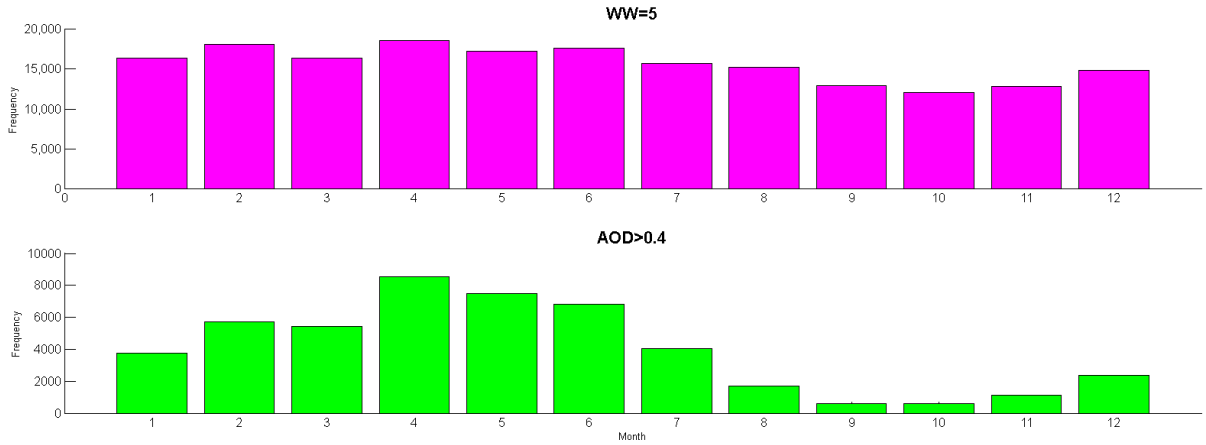

Figure 4. Monthly frequency of code 5 and AOD> 0.4 (0.4 average value)

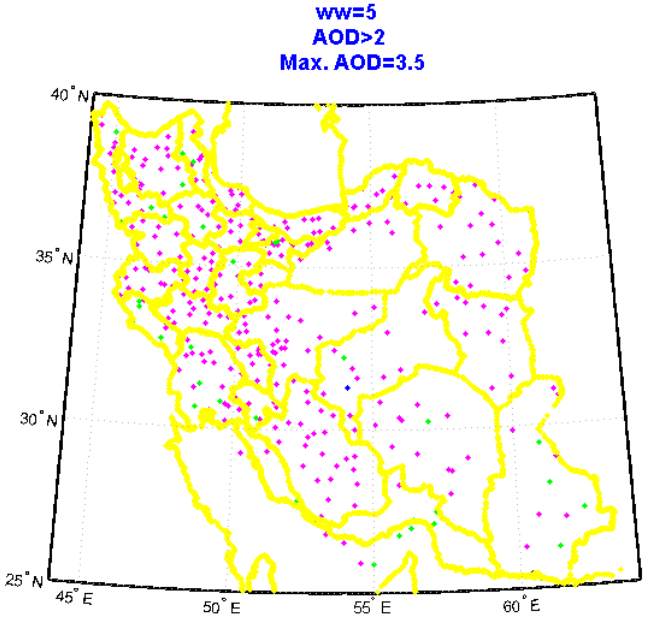

Figure 5. Scattering code 5 (Pink), AOD>2 (Green) and AOD=3.5 (Blue)

The frequency of AOD>0.4 (0.4 average value) in the first half of the year (especially July) was higher than that of the second half of the year. Given the lack of moisture and rainfall in the first half of the year, it is logical to observe an increasing trend in air pollution. The values AOD>2 were more common in the border cities of the northwest, west, and southwest of the country. Contaminants from neighboring countries may be transmitted to Iran (Figures 3, 4, and 5). This phenomenon was also observed in the islands of the Persian Gulf and the Gulf of Oman. Despite the relative humidity of 71% on 2008/07/22, August in the coastal city of Konarak recorded the highest amount of aerosol optical depth in code 5, which was 3.5. It seems that the invasion of spray particles and marine salts from the Gulf of Oman and the combination of these particles with the available moisture and water vapor droplets contributed to the increase in AOD. The desert and dry city of Gariz (Yazd), with a low relative humidity of 20%, had the highest amount of aerosol optical depth in code 5, which was reported at 3.5 on 2008/04/07. Seemingly, environmental factors and surrounding sand fields or desert and desert salts were the reasons behind the increase in AOD in this city.

The blizzard phenomenon, code 10 monitoring, was usually reported along with the phenomena of rain and snow. The values of AOD>0.25 (0.25 average value) were usually higher in the second half of the year compared to the first half of the year. For instance, the rainfall, along with the relative humidity of 91% increased the AOD value to 3.5 in the city of

Dargaz on 2017/12/01. The combination of water droplets and seasonal rainfall may have increased AOD. 4.5% of large 2.6<=AOD<= 2.7 is in code 10.

Lightning and thunder (codes 13 and 17) were well correlated with the amount of AOD. Lightning and thunderstorms are associated with other atmospheric phenomena, such as rain and snow. The value of 2.9, for example, was recorded for AOD on 2009/04/16 in the city of Jolfa. Of note, rapid weather changes (turbulence) with rain and rainstorm in the spring also occurred in this city on the same date. In some cases, prior to lightning, code 5 (air pollution) also occurred which can be referred to Konarak on 2008/07/15 when the AOD value reached 1.9.

The type of rain and snow is important and effective in the amount of AOD, and the formation of coarser particles led to larger AOD, which is consistent with the scientific research of other researchers such as (Levy et al., 2009) and (Chu et al., 2003). Rainstorms and snow (low, medium, and heavy) increase the amount of aerosol optical depth. For example, codes 91 and 95 were reported in the city of Sardasht on 2009/06/18, when the AOD value of 2.99 was measured. The coastal and port cities also have large amounts of AOD in times of high humidity and no rain. A relevant example would be the port of Mahshahr on 2013/11/24, when the AOD was 2.6 and the relative humidity was 89%. Regarding the industrial nature of this city and its proximity to the Persian Gulf, it seems that the combination of industrial and chemical pollutants, suspended particles of sea spray, and air humidity affect the amount of AOD. The values of AOD>0.31 (0.31 average value) of code 95 were higher in the western and southwestern regions of the country (Figure 6). Rainfall and rainstorms in humid and forested areas in May also increased the amount of AOD, which can be referred to as 2.85 on 2013/05/17 in the city of Kojour, Mazandaran. Snow codes (light, moderate, and severe) are also associated with other weather phenomena and have been reported at different hours of monitoring. For example, the snow phenomenon was accompanied with heavy fog in the winter of 2017/02/02 in the city of Ilam and the AOD value peaked at3.5. In this city, heavy rainfall and the formation of larger droplets increase the amount of AOD and their correlation has been proven in scientific studies (Alam et al., 2010). 0.1% of large $1.3 <= AOD <= 1.4$ values are present in codes 60 to 69 (code 62). Furthermore, 0.14% of large $1.4 <= AOD <= 1.5$ values is in codes 80 to 89 (code 80), and 8.3% of large $2.9 <= AOD <= 3.0$ are present in codes 90 to 99 (code 91).

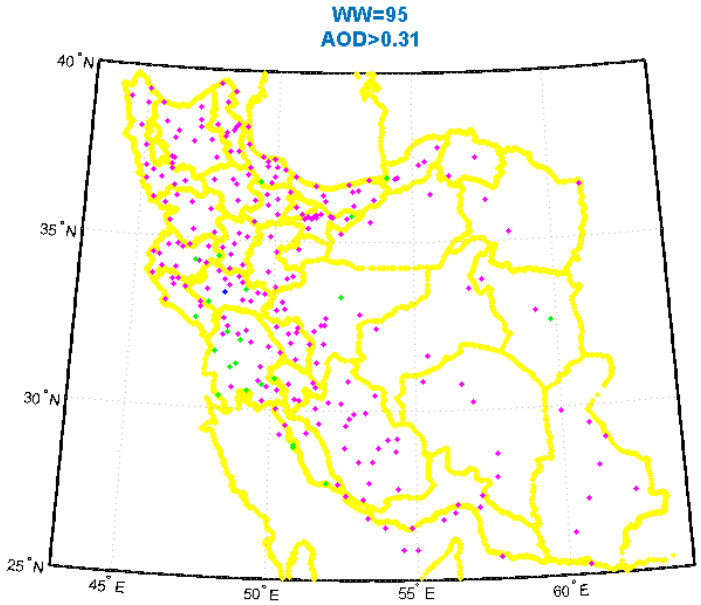

Figure 6. Scattering code 95 (Pink) and AOD>0.31 (0.31 average value) (Green) 4

The results of the present study are summarized as follows:

1. AOD values at 550 nm are suitable and reliable for studying aerosols over Iran. MODIS AOD data is useful for recognizing and detecting meteorological phenomena (codes 00 to 99). The value of AOD varies with the season, place, and meteorological phenomena in Iran.
2. The large amounts of AOD are not caused by dust storms, but other atmospheric phenomena such as rain and snow, rainstorm (shower), water vapor, and boundary layer pollutants play important roles. The existence of factory pollution in industrial and large cities, type of rainfall (such as heavy rain, thunderstorms, lightning, and shower), air stability, and accumulation of pollutants will increase the amount of AOD.
3. Water vapor and air humidity are of great importance in the boundary layer; thus, increasing and decreasing them leads to an increased amount of AOD. In coastal cities or forested areas and ports in southern Iran, the presence of high relative humidity (no rainfall) along with hot weather cause the fine water drop lets to form larger droplets which will increase the amount of AOD. In arid and desert cities, without rain and low relative humidity, the amount of AOD increases, which seems that environmental factors in these areas cause air pollution and an increase in the amount of AOD.
4. Among the weather codes 00 to 99, the highest frequency percentage of 0<=AOD<=3.5 was related to codes 5 and 6. The frequency of values AOD>0.4 (0.4 average value) related to code 5 in the first half of the year (especially July) was higher than that of the second half of the year. Analysis of code 5 and AOD values in Mashhad showed that this phenomenon was associated with very calm winds (2 to 3 meters per second), low horizontal visibility and temperature inversion (inversion). The values of AOD>0.3 (0.3 average value) related to code 4 in June and July were higher than that of other months. Values of AOD>0.25 (0.25 average value) belonging to code 10 in the second half of the year were more than the first half of the year. Values of AOD>0.31 (0.31 average value) related to code 95 were higher in the western and southwestern regions of Iran.

In summary, meteorological phenomena with natural, industrial, and fabricated sources can be studied with the help of AOD data in the MODIS sensor band 4 at 550 nm (Kaufman et al., 2005). Urban and industrial pollution, fine particles suspended in the sea, desert sand and soil, smoke from forest fires, and factory soot increase the amount of AOD (Alam et al., 2010), (Chu et al., 2003). Furthermore, the combination of these particles and pollutants is closely associated with increased AOD. The amount of AOD is directly related to meteorological phenomena (short-term or long-term) such as cloudiness, changes in humidity, lightning, thunderstorms, and heavy rainfall. The use of MODIS AOD is an appropriate and useful approach to studying air pollution quality control in cities (Hsu et al., 2013).

References

Alam K, Iqbal MJ, Blaschke T, Qureshi S, Khan G. 2010. Monitoring spatio-temporal variations in aerosols and aerosol–cloud interactions over Pakistan using MODIS data. Advances in Space Research, 46(9), pp.1162-1176.

Bahram Vash Shams Sh, Mohammadzadeh A. 2013. Investigation of optical properties and dust particle size and their dependencies using AERONET data, Journal of Advanced Applied Geology; Winter 2013; No. 10

Bilal M, Qiu Z, Campbell JR, Spak SN, Shen X, Nazeer M. 2018. A new MODIS C6 Dark Target and Deep Blue merged aerosol product on a 3 km spatial grid. Remote Sensing, 10(3), p.463.

Chu DA, Kaufman YJ, Zibordi G, Chern JD, Mao J, Li C, Holben BN. 2003. Global monitoring of air pollution over land from the Earth Observing System-Terra Moderate Resolution Imaging Spectroradiometer (MODIS). Journal of Geophysical Research: Atmospheres, 108(D21).

Ensafi Moghaddam T. 2021. Investigation of Aerosol Optical Depth (AOD) Index in Dust Events in Southwestern Iran, Nature of Iran, 5(6), 55-67

Fan A, Chen W, Liang L, Sun W, Lin Y, Che H, Zhao X. 2017. Evaluation and comparison of long-term MODIS C5. 1 and C6 products against AERONET observations over China. Remote Sensing, 9(12), 1269.

Gkikas A, Hatzianastassiou N, Mihalopoulos N. 2009, September. Aerosol events in the broader Mediterranean basin based on 7-year (2000–2007) MODIS C005 data. In Annales Geophysicae (Vol. 27, No. 9, pp. 3509-3522). Copernicus GmbH.

Hsu NC, Jeong MJ, Bettenhausen C, Sayer AM, Hansell R, Seftor CS, Huang J, Tsay SC. 2013. Enhanced Deep Blue aerosol retrieval algorithm: The second generation. Journal of Geophysical Research: Atmospheres, 118(16), pp.9296-9315.

http://modis-atmos.gsfc.nasa.gov/MOD04_L2/index.html.(MODIS Atmosphere Aerosol Product 2021).

https://irimo.ir/far/index.php (I.R.OF IRAN Meteorological Organization 2021).

Ichoku C, Kaufman YJ, Remer LA, Levy R. 2004. Global aerosol remote sensing from MODIS. Advances in Space Research, 34(4), 820-827.

Kaufman YJ, Tanré D, Remer LA, Vermote EF, Chu A, Holben BN. 1997. Operational remote sensing of tropospheric aerosol over land from EOS moderate resolution imaging spectroradiometer. Journal of Geophysical Research: Atmospheres, 102(D14), 17051-17067.

Kaufman YJ, Boucher O, Tanré D, Chin M, Remer LA, Takemura T. 2005. Aerosol anthropogenic component estimated from satellite data. Geophysical Research Letters, 32(17).

Klingmüller K, Pozzer A, Metzger S, Stenchikov GL, Lelieveld J. 2016. Aerosol optical depth trend over the Middle East. Atmospheric Chemistry and Physics, 16(8), 5063-5073.

Kucienska B, Raga GB, Altaratz O, Koren I, Quintanar A. 2013. The relation between aerosol optical depth and lightning from the tropics to the mid-latitudes. In The 5th Symp. on Aerosol-Cloud-Climate Interactions. Austin, TX: American Metrological Society.

Levy RC, Remer LA, Tanré D, Mattoo S, Kaufman YJ. 2009. Algorithm for remote sensing of tropospheric aerosol over dark targets from MODIS: Collections 005 and 051: Revision 2; Feb 2009.
MODIS algorithm theoretical basis document.

Levy RC, Remer LA, Kleidman RG, Mattoo S, Ichoku C, Kahn R, Eck TF. 2010. Global evaluation of the Collection 5 MODIS dark-target aerosol products over land. Atmospheric Chemistry and Physics, 10(21), 10399-10420.

Levy RC, Mattoo S, Munchak LA, Remer LA, Sayer AM, Patadia F, Hsu NC. 2013. The Collection 6 MODIS aerosol products over land and ocean. Atmospheric Measurement Techniques, 6(11), 2989- 3034.

Li J, Ge X, He Q, Abbas A. 2021. Aerosol optical depth (AOD): spatial and temporal variations and association with meteorological covariates in Taklimakan desert, China. PeerJ, 9, e10542.

Masoodian SA. 2011. Iran's Weather; Sharia Toos Publications; Mashhad.

Rayegani B, Kheirandish Z. 2017. Utilization of time series of satellite data to validate the identified centers of dust production in Alborz province; Journal of Spatial Analysis of Environmental Hazards; Fourth year; No. 4; Winter 2017

Remer LA, Kaufman YJ, Tanré D, Mattoo S, Chu DA, Martins JV, Holben BN. 2005. The MODIS aerosol algorithm, products, and validation. Journal of atmospheric sciences, 62(4), 947-973.

Sayer AM, Hsu NC, Bettenhausen C, Jeong MJ. 2013. Validation and uncertainty estimates for MODIS Collection 6 “Deep Blue” aerosol data. Journal of Geophysical Research: Atmospheres, 118(14),
7864-7872.

Sayer AM, Hsu NC, Bettenhausen C, Jeong MJ, Meister G. 2015. Effect of MODIS Terra radiometric calibration improvements on Collection 6 Deep Blue aerosol products: Validation and Terra/Aqua consistency. Journal of Geophysical Research: Atmospheres, 120(23), 12-157.

Soleimani A, Mohammad Asgari H, Dadallahi S, Alamizadeh H, Khazaei SH. 2015. Optical Depth Evaluation of MODIS Satellite Images in the Persian Gulf, Iranian Journal of Marine Science and Technology; Winter 2015; Volume 14; No. 4.

Thomas MA, Devasthale A, Tjernström M, Ekman AM. 2019. The relation between aerosol vertical distribution and temperature inversions in the Arctic in winter and spring. Geophysical Research Letters, 46(5), 2836-2845.

Wahab AM, Sarker MLR. 2014, February. Aerosol retrieval algorithm for the characterization of local aerosol using MODIS L1B data. In IOP conference series: earth and environmental science (Vol. 18,No. 1, p. 012098). IOP Publishing.

Wei J, Sun L. 2016. Comparison and evaluation of different MODIS aerosol optical depth products over the Beijing-Tianjin-Hebei region in China. IEEE Journal of Selected Topics in Applied Earth Observations and Remote Sensing, 10(3), 835-844.

Wei J, Sun L, Huang B, Bilal M, Zhang Z, Wang L. 2018. Verification, improvement and application of aerosol optical depths in China Part 1: Inter-comparison of NPP-VIIRS and Aqua-MODIS. Atmospheric Environment, 175, 221-233.

Wei J, Li Z, Sun L, Peng Y, Liu L, He L, Qin W, Cribb M. 2020. MODIS Collection 6.1 3 km resolution aerosol optical depth product: global evaluation and uncertainty analysis. Atmospheric Environment, 240, p.117768.

Xin J, Gong C, Liu Z, Cong Z, Gao W, Song T, Pan Y, Sun Y, Ji D, Wang L, Tang G. 2016. The observation-based relationships between PM2. 5 and AOD over China. Journal of Geophysical Research: Atmospheres, 121(18), pp.10-701.